Dynamic Interconversion of Amorphous Microparticles and Crystalline Rods in Salen-Based Homochiral Infinite Coordination Polymers

You-Moon Jeon, Jungseok Heo, and Chad A. Mirkin*

*Department of Chemistry and the International Institute for Nanotechnology, Northwestern University,
2145 Sheridan Road, Evanston, Illinois 60208-3113*

Received February 16, 2007; E-mail: chadnano@northwestern.edu

Nano- and micrometer-sized particles of organic polymers and inorganic materials play an important role in many applications, including catalysis, optics, biosensing, and data storage.[1] As an alternative, our group and others recently have developed synthetic approaches for the preparation of amorphous particles from infinite metal-organic coordination polymers, which are based on the coordination chemistry of late transition metal ions and polydentate organic building blocks.[2,3] The infinite coordination polymer (ICP) particles offer a high degree of tailorability through the choice of transition metal connectors and predefined functional organic precursors which have useful chemical and physical properties.[2,3] However, the amorphous nature of ICP particles, in contrast to the well-defined crystalline metal-organic frameworks (MOFs),[4] prohibit a detailed understanding of the structural connectivity and transition metal coordination environments of these systems due to their inability to diffract X-rays. Herein, we wish to report a new class of salen-based homochiral ICP particles and the discovery that judicious choice of solvent can be used to drive the amorphous spherical particles into rod-shaped crystalline structures that can be fully characterized by X-ray crystallography. These data provide key structural information about the likely molecular connectivity of the precursors that make up the amorphous ICP microparticles.

Acid-functionalized salen ligands were synthesized according to literature procedures and used for the preparation of ICP particles and crystalline rods.[5] Spherical particles **2a** and **2b** were prepared by slow diffusion of diethyl ether into a precursor pyridine solution consisting of a 1:1 mixture of $Ni(OAc)_2 \cdot 4H_2O$ and metallo-salen precursors, H_2-**1a** and H_2-**1b**, respectively (Scheme 1).

The particle formation reaction is completely reversible, as evidenced by the formation of a clear solution upon addition of excess pyridine to the particles in their dried form.[2] ^{1}H NMR and UV−vis spectra confirm the re-formation of the metallo-salen precursors. The morphology of the microscale ICP particles was characterized by optical microscopy (OM) and field-emission scanning electron microscopy (FE SEM) (Figure 1). The images show spherical structures with an average diameter of 2.69 ± 0.13 and 5.70 ± 0.84 μm for **2a** and **2b**, respectively. The particle size was further studied by dynamic light scattering (DLS), and the DLS-determined mean particle size values of 2.46 μm for **2a** and 5.52 μm for **2b** are in good agreement with the SEM determined values. The chemical compositions of **2a** and **2b** were characterized by energy dispersive X-ray (EDX) spectroscopy and elemental analyses and are consistent with formation of the 1:1 structure derived from the metallo-salen and metal ion precursors.

Infrared spectra taken of the microparticles show that the carboxylate groups are coordinated to metal ions, as evidenced by a shift of the carboxylate stretching frequency from 1683 cm^{-1} in the protonated metallo-salen precursor H_2-**1a** to 1531 (ν_{anti}) and 1437 cm^{-1} (ν_{sym}) for **2a**. These values compare very well with the stretching frequencies for $Ni(OAc)_2 \cdot 4H_2O$ at 1535 and 1422 cm^{-1},
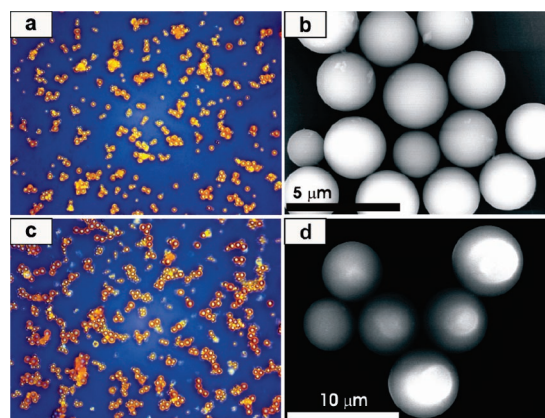
Figure 1. OM and SEM images of spherical ICP particles: (a) and (b) for **2a**, (c) and (d) for **2b**.

Scheme 1. Synthesis of Salen-Based Microparticles and Their Dynamic Solvent-Triggered Crystallization Process: (a) Pyridine/Ether, (b) Pyridine, (c) MeOH, (d) Pyridine/MeOH, (e) Pyridine
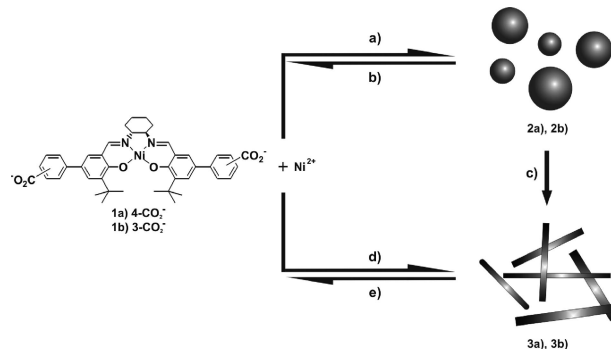
consistent with η^1-coordination of the carboxylate groups to the Ni centers through their anionic O atoms. The IR spectra of ligand H_2-**1b** and microparticle **2b** show similar trends.

Interestingly, when microparticles **2a** and **2b** were completely dried under vacuum, they retained their spherical shapes, but when methanol was added to them, they transformed in the solid state into crystalline rod-shaped structures. Note the particles and the rod-shaped products are not soluble in methanol. This solid-state transformation could be followed by analyzing samples taken from the reaction mixture as a function of time over a ~60 min time period (Figure 2). The initial microparticles **2a** have a smooth surface (Figure 2a). However, in the presence of methanol, the surface morphology of the particle becomes ruffled as the solvent begins to penetrate the particle (Figure 2b). Then, sharp needles begin to grow from the surface (Figure 2c), and eventually the particles turn into crystalline rods **3a** (Figure 2d).

Interestingly, the crystalline rods **3a** can be transformed into the microparticles **2a** again by first dissolving the rods in pyridine and
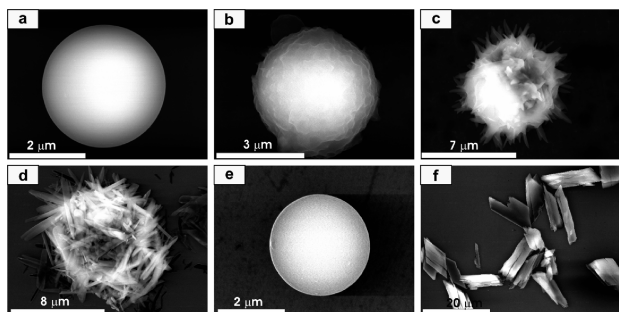
Figure 2. Representative SEM images monitoring the transformation of microparticles **2a** to crystalline rods **3a**. (a) Particle **2a** grown from the precursor solution, (b) early intermediate (5 min), (c) intermediate at a later stage (30 min), (d) crystalline rods **3a**, (e) particle grown by first dissolving the crystalline rods **3a** with pyridine and then exposing to ether by vapor diffusion, and (f) crystalline products **3a** grown from the pyridine precursor **1a** solution, Ni(OAc)$_2$·4H$_2$O, and methanol.

then slowly diffusing ether into the solution (Figure 2e). The dissolution of the crystalline rods with pyridine results in the re-formation of the salen and metal ion precursors as confirmed by ^{1}H NMR and UV–vis spectroscopy. Taken together, these processes make the entire cycle between precursors, microparticles, and rod-shaped crystalline structures pseudo-reversible (Scheme 1). In other words, the crystalline rods do not go back to the amorphous particles without redispersing the metallo-salen and metal ion precursors in solution.

The crystalline product **3a** can be prepared directly by slow diffusion of methanol into the pyridine solution of precursors, as well (Figure 2f). However, the crystalline rods made from the amorphous microparticles by the methanol-triggered process are more uniform and have higher aspect ratios than those made from the direct crystallization in pyridine method. We also investigated the IR spectra of the crystalline products **3a** and **3b**. The carboxylate stretching frequencies of **3a** at 1531 and 1439 cm^{-1} are comparable to those for the amorphous microparticle sample **2a** (1531 and 1437 cm^{-1}) and Ni(2,6-DMB)$_2$(py)$_2$(EtOH)$_2$ (1555 and 1400 cm^{-1}),[6] which suggest that they have similar metal carboxylate connectivities. Compound **3b** shows similar trends (Supporting Information).

Significantly, a single crystal of **3a** suitable for an X-ray diffraction study was grown by adding methanol to a pyridine solution of the salen and metal ion precursors. X-ray crystallography shows that the structure of **3a** consists of a one-dimensional coordination polymer (Figure 3). The Ni ions exhibit a distorted octahedral coordination geometry with two *trans*-carboxylate (Ni–O$_{avg}$ = 2.05 Å), two *cis*-pyridine (Ni–N$_{avg}$ = 2.10 Å), and two *cis*-methanol (Ni–O$_{avg}$ = 2.13 Å) groups. The coordination geometry around the Ni is similar to that observed for the model monomeric Ni(py)$_2$(OAc)$_2$(H$_2$O)$_2$ complex.[7] The IR and XRD spectra of the single crystal were superimposable with those for crystalline rods of **3a** grown from the polymer particles, showing that crystalline materials grown the different ways are chemically identical from composition ratio and connectivity standpoints. Note that the major difference between the ICP spherical particles and crystalline rods is the coordination of methanol to the Ni atoms in
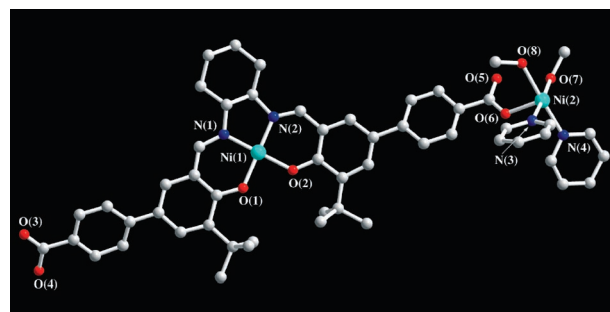
Figure 3. X-ray structure of crystalline **3a** (one of the two repeating units: gray, carbon; blue, nitrogen; red, oxygen; sky blue, nickel). Hydrogen atoms and solvent molecules have been omitted for clarity.

the latter structure. This is likely the driving force for the amorphous to crystalline transformation.

In conclusion, this paper describes a new class of homochiral salen-based ICPs and the discovery of a novel and pseudo-reversible solvent-induced crystallization process. The solvent, methanol in this case, induces such a transformation through a change in the coordination environment around the metal bridging the metallo-salen portion of the complex. This novel transformation has allowed us to use X-ray methods to structurally characterize the crystalline product and through spectroscopic comparisons better understand the connectivity and structure of the amorphous ICP particle precursor. To the best of our knowledge, this is the first single-crystal X-ray diffraction data for polymeric materials that derive from the amorphous ICPs.

Supporting Information Available: Experimental details, characterization of microparticles and rods, and X-ray data for **3**. This material is available free of charge via the Internet at http://pubs.acs.org.

References

(1) (a) Bell, A. T. *Science* **2003**, *299*, 1688. (b) Blanco, A.; Chomski, E.; Grabtchak, S.; Ibisate, M.; John, S.; Leonard, S. W.; Lopez, C.; Meseguer, F.; Miguez, H.; Mondia, J. P.; Ozin, G. A.; Toader, O.; van Driel, H. M. *Nature* **2000**, *405*, 437. (c) Bruchez, M.; Moronne, M.; Gin, P.; Weiss, S.; Alivisatos, A. P. *Science* **1998**, *281*, 2013. (d) Cao, Y. C.; Jin, R.; Mirkin, C. A. *Science* **2002**, *297*, 1536. (e) Sun, S.; Murray, C. B.; Weller, D.; Folks, L.; Moser, A. *Science* **2000**, *287*, 1989. (f) Wang, J.; Gudiksen, M. S.; Duan, X.; Cui, Y.; Lieber, C. M. *Science* **2001**, *293*, 1455.

(2) (a) Oh, M.; Mirkin, C. A. *Nature* **2005**, *438*, 651. (b) Oh, M.; Mirkin, C. A. *Angew. Chem., Int. Ed.* **2006**, *45*, 5492.

(3) (a) Maeda, H.; Hasegawa, M.; Hashimoto, T.; Kakimoto, T.; Nishio, S.; Nakanishi, T. *J. Am. Chem. Soc.* **2006**, *128*, 10024. (b) Park, K. H.; Jang, K.; Son, S. U.; Sweigart, D. A. *J. Am. Chem. Soc.* **2006**, *128*, 8740. (c) Sun, X.; Dong, S.; Wang, E. *J. Am. Chem. Soc.* **2005**, *127*, 13102.

(4) (a) Bradshaw, D.; Claridge, J. B.; Cussen, E. J.; Prior, T. J.; Rosseinsky, M. J. *Acc. Chem. Res.* **2005**, *38*, 273. (b) Yaghi, O. M.; O'Keeffe, M.; Ockwig, N. W.; Chae, H. K.; Eddaoudi, M.; Kim, J. *Nature* **2003**, *423*, 705. (c) Seo, J. S.; Whang, D.; Lee, H.; Jun, S. I.; Oh, J.; Jeon, Y. J.; Kim, K. *Nature* **2000**, *404*, 982.

(5) Jeon, Y.-M.; Heo, J.; Mirkin, C. A. *Tetrahedron Lett.* **2007**, *48*, 2591.

(6) Erre, L. S.; Micera, G.; Gulinati, B.; Cariati, F. *Polyhedron* **1992**, *11*, 101.

(7) Drew, J.; Hursthouse. M. B.; Thornton, P. *J. Chem. Soc., Dalton Trans.* **1972**, 1658.

JA071046W